THE EFFECT OF NUMBER OF FABRIC ON CFRP-FABRIC HYBRID COMPOSITE IMPACT SHIELD PERFORMANCE

J. B. Moon[1], G. S. Son[1], Y. R. Park[1], C. G. Kim[1]*
[1] Division of Aerospace Engineering, School of Mechanical, Aerospace and System Engineering, Korea Advanced Institute of Science and Technology, Daejeon, Korea
* Corresponding author(cgkim@kaist.ac.kr)

Keywords: *LEO space, MMOD, hypervelocity impact, hybrid shield, composite*

1 Introduction

Low earth orbit (LEO) which is 200 km to 6400 km altitude has many spacecrafts. There are many harsh environmental factors which can degrade material properties and damage the space structure. The main constituents which can degrade the material properties of composites are high vacuum, atomic oxygen(AO), ultra-violet light(UV light) and thermal cycling. Another harsh environmental factor is micro-meteoroid and orbital debris(MMOD). MMOD is different from the previous 4 constituents. It does not contribute to the erosion of polymer materials. However, it occasionally collides with spacecraft and damages the spacecraft severely. Hypervelocity impact with orbital debris and micro-meteoroids is highlighted as a severe threat to spacecraft due to their tremendously high velocity (5~70 km/s). Even with their small size, MMOD can cause critical damages to spacecraft when it is impacted and micrometeoroids and orbital debris (MMOD). These impacts can cause the degradation of the function of spacecraft, mission failure and malfunction of space vehicle. The threat of the MMOD is increased as the population of MMOD is increased [2,3]. Therefore, the shielding system to protect the spacecrafts from MMOD is needed.

As a shield for spacecrafts, Whipple shields are widely studied and used. It can reduce the weight of the shielding system itself, but it can cause the increase of a volume due to large standoff.

In this study, a new concept of shielding system which has compact size, light weight and high energy absorbing rate is suggested. And the effect of number of intermediate fabric plies of hybrid shielding system was studied by using 2-stage gas gun.

2 Hybrid Sandwich Shielding System

2.1 Concept of Shield

The hybrid sandwich shielding system consists of two bumper plates and one intermediate fabric as shown in Fig.1. The first bumper is made up of carbon fiber reinforced plastic (CFRP) which has good energy absorbing rate and light weight. And the Kevlar fabric is added as interlayer with unrestrained inplane boundary condition. Finally the rear plate is made up of polymer plate which is easily penetrated before the failure of Kevlar.

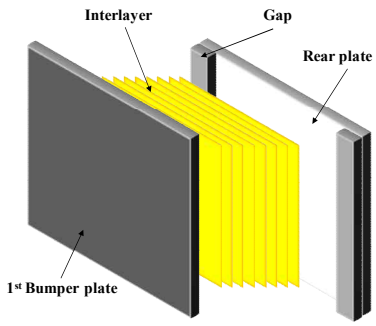

Fig.1. Schematic of CFRP-Kevlar hybrid shield.

2.2 Energy absorbing mechanism

The main mechanism of this shield is fabric pull-out from the penetration hole of the rear wall. The schematic diagram of the impact process is shown in Fig. 2. When projectile hit the first bumper, the penetration is firstly occurred at the relatively weak real polymer plate. And the intermediate layer Kevlar is pulled out through the hole of rear plate because it is not fixed anywhere. However new boundary condition is created at the rear wall hole. As the projectile goes on, the volume of fabric and friction force in the hole are increased. But the increase rate of reaction force in the hole is relatively slower than that of fixed one. Therefore

the energy absorbing occurs for much long time and the total absorbed energy is increased.

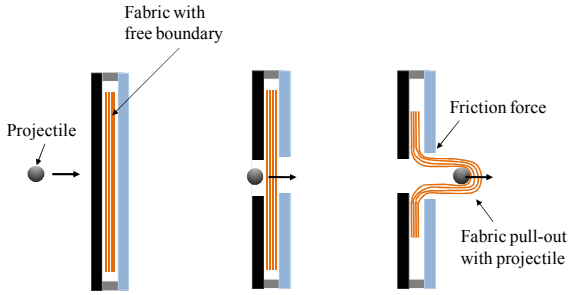

Fig.2. Energy absorbing process of hybrid shield (fabric pull-out mechanism).

3 Experiment

3.1 Specimen preparation

Same front and rear bumper plate were used during experiment. The 1.8mm CFRP was prepared. It was made up of CU125NS with stacking sequence of $[0/\pm45/90]_{2s}$. And the 2mm poly methylmetaacrylate (PMMA) was used as rear wall. The Kevlar KM2 was used as interlayer. And 3 different number of ply were used to verify the effect of number of interlayer plies.

Table 1. Description of specimen

Denotation	1st bumper	Intermediate layer	Rear plate
CKPA4	CFRP (1.8mm)	Kevlar KM2 4 plies	PMMA (2mm)
CKPA6	CFRP (1.8mm)	Kevlar KM2 6 plies	PMMA (2mm)
CKPA8	CFRP (1.8mm)	Kevlar KM2 8 plies	PMMA (2mm)

3.2 Hypervelocity impact simulation equipment

2-stage gas gun was used to simulate the hypervelocity impact with space debris. Fig. 3 shows the picture and the schematic diagram of 2-stage gas gun. The 5.56mm diameter spherical aluminum alloy (Al2017) ball was used as a projectile. The weight of aluminum ball is 0.25 ±0.001g. The aluminum projectile was launched with average velocity of 1±0.05 km/s by using the gas gun.

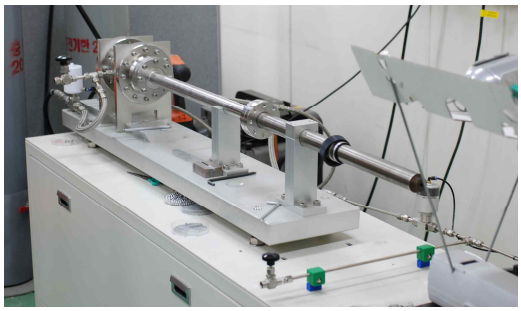

(a) Photo of 2 stage gas gun.

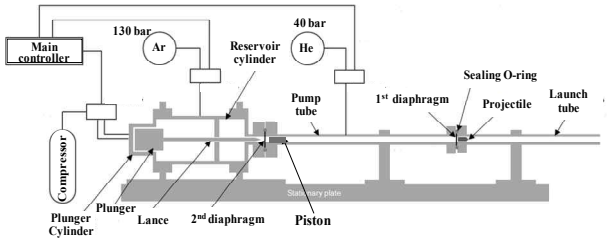

(b) Schematic picture of 2 stage gas gun.

Fig.3. 2-stage light gas gun.

3.3 Velocity measurement and calculation of energy absorption

The velocity before and after impact were measured to calculate the difference in the kinetic energy and finally determine the absorbed impact energy by the structure. Negligible factors such as the heat produced from friction during impact, and acoustic energy were discarded and Eq. 1 was used.

$$E = \frac{1}{2} m \left(V^2_{initial} - V^2_{residual} \right) - E_{air} \quad (1)$$

In the above equation, m is the mass of the projectile, $V_{initial}$ is the projectile velocity before impact, and $V_{residual}$ is the velocity after impact. E_{air} is the energy loss due to the air since the projectile is not passing through vacuum but the atmosphere of 1 atm. E_{air} was determined experimentally, and the result showed that depending on the initial projectile velocity it was linear. E_{air} was concisely described as Eq. 2.

$$E_{air} = \frac{1}{2}(0.0183\, V_{initial} - 2.89) + \frac{1}{2}(0.0183\, V_{residual} - 2.89) \quad (2)$$

2 chronographs were employed to measure the initial velocity and velocity after impact. The chronograph

can measure up to 2km/s, and the 2 devices were installed before and after the target fixture.
A stainless steel case was manufactured and set with a 4 edge fixed constraint condition as shown in Fig. 4. This set up was then installed on the target fixture between the 2 chronographs as shown in Fig. 4. The exposed specimen area during the impact test is 100×100mm.

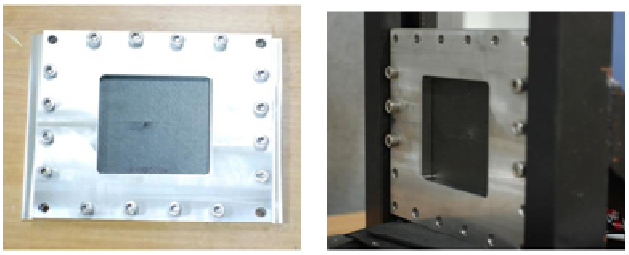

Fig. 4. Target fixture.

4 Results and discussion

4.1 Hypervelocity impact test result

Fig. 5 shows the energy absorbing rates of CKPA8, CKPA6, and CKPA4. As can be seen in the figure, CKPA8 and CKPA6 shows similar energy absorbing rates. But the interlayer plies of fabric was smaller than 4 layers, the energy absorbing rate was decreased.

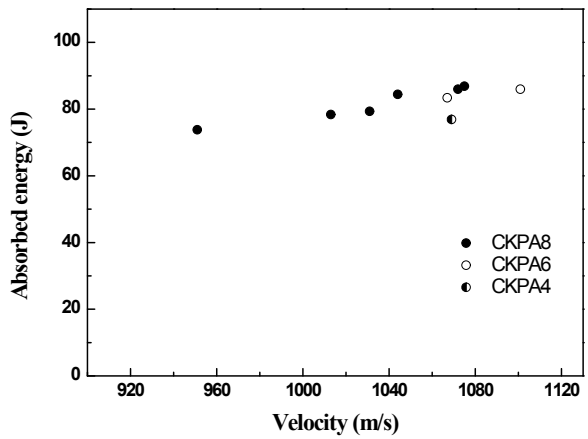

Fig. 5. Absorbed energy of CKPA8, CKPA6 and CKPA4.

The individual components energy absorbing rate was calculated. This was then compared to the energy absorbing rate of the hybrid composite shield. Table 2 shows the shield energy absorbing rate CKPA with different number of fabric. It shows that the all the CKPA had an energy absorption rate higher than that of the individual components sum by about 8.91%, 7.92% and 4.19% for CKPA8, CKPA6 and CKPA4 respectively. This shows that by using unrestrained boundary added fabric, a new energy absorbing mechanism occurred. And it needed to have enough number of fabrics as intermediate layer.

Table 2. Energy absorbing rate of CKPA hybrid composite shield with different number of fabric plies and sum of individual component

	Individual component				Hybrid type
	CFRP	KM2	PMMA	Sum	
CKPA8	39.80J	10.38J	21.55J	71.73J	**78.12J (8.91%)**
CKPA6	39.80J	7.79J	21.55J	69.14J	**75.09J (7.92%)**
CKPA4	39.80J	5.19J	21.55J	66.54J	**69.45J (4.19%)**

4.2 Penetration shape of hybrid composite shield

The failure mode around the penetration hole for the CKPA design using the PMMA rear plate is shown in Fig. 6.

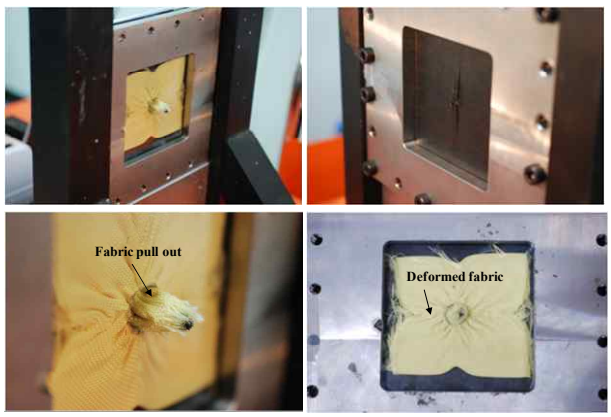

Fig. 6. Fracture shape of hybrid CFRP_Kevlar_MMA shield (fabric pull-out and deformed fabrics).

The backside view image shows that a penetration hole of about diameter 9mm occurred in the PMMA

plate and the fabric is clearly protruding. The rupture of the fabric fiber at the penetration area is evident due to the tensile load. There was no rupture in the last ply due to compressive pressure, and overall large amounts of fabric pull-out occurred. This leads to the conclusion that fabric rupture did not occur from the high compressive pressure at early hypervelocity impact, but failure occurred during pull-out through the penetration hole in the rear plate. As the fabric pull-out progresses through the hole, the volume within the hole increases which in turn increases the binding by friction. This leads to the increase in tensile load acting on the front surface of the projectile. The increasing tensile stress reaches ultimate strength and the fabric finally fails. This phenomenon shows that the fabric pull out mechanism proposed in this study was clearly realized.

The shapes of the protruded fabric with different intermediate layer were shown in Fig. 7. As shown in figure, much more pull-out of fabric was observed as the number of the fabric was increased. As the number of the fabric increased, the load, which the fabric can carry, was increased and penetration was occurred much later than that of the hybrid composite shield with less intermediate layer.

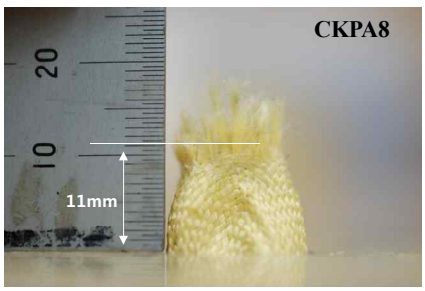

(a) Protruding shape of CKPA8

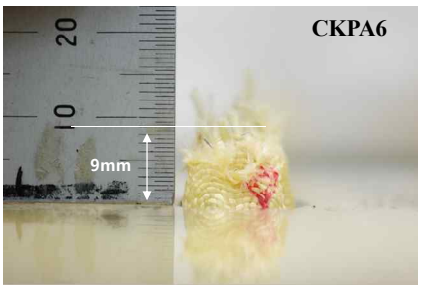

(b) Protruding shape of CKPA6

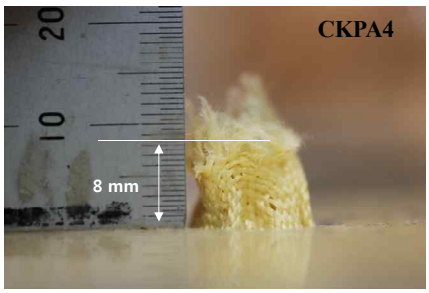

(c) Protruding shape of CKPA4

Fig. 7 Shape of the protruded fabric of hybrid composite shield.

5 Conclusion

In this paper, the hybrid sandwich composite shield with unrestrained boundary fabric was studied to improve the energy absorbing rate by using new additional energy absorbing mechanism namely the fabric pull-out. By using the PMMA as the rear plate, the fabric pull-out mechanism was realized and the energy absorbing was increased due to this. The effect of the number of ply of intermediate layer fabric was also studied. By using much more plies of fabric the energy absorbing rate was increased because the failure loads was increased as the increase of fabric plies. The fabric pull-out can occurred much longer time and energy was absorbed for long time.

Acknowledgements

The present work was supported by National Research Foundation of Korea (Project Nos. 2009-0079968). The authors would like to thank for the financial support.

References

[1] J. H. Han "*Low-Earth-Orbit Space Environment Characteristics of Nano-filler Reinforced Polymer Matrix Composites*". Doctorial thesis 2005.

[2] Y. L. Xu, M. Horstman, P. H. Krisko, J. C. Liou, M. Matney, E. G. Stansbery, C. L. Stokely and D. Whitlock "*Modeling of LEO orbital debris populations for ORDEM2008*". *Advances in Space Research*, Vol. 43, pp. 769–782, 2009.

[3] J. C. Liou, N. L. Johnson, N. M. Hill "*Controlling the growth of future LEO debris populations with active debris removal*". *Acta Astronautica*, Vol.66, pp. 648-653, 2010.